Direct detection of Pb in urine and Cd, Pb, Cu, and Ag in natural waters using electrochemical sensors immobilized with DMSA functionalized magnetic nanoparticles

Wassana Yantasee,* Kitiya Hongsirikarn, Cynthia L. Warner, Daiwon Choi, Thanapon Sangvanich, Mychailo B. Toloczko, Marvin G. Warner, Glen E. Fryxell, R. Shane Addleman and Charles Timchalk

Received 23rd July 2007, Accepted 15th December 2007
First published as an Advance Article on the web 1st February 2008
DOI: 10.1039/b711199a

Urine is universally recognized as one of the best non-invasive matrices for biomonitoring exposure to a broad range of xenobiotics, including toxic metals. Detection of metal ions in urine has been problematic due to the protein competition and electrode fouling. For direct, simple, and field-deployable monitoring of urinary Pb, electrochemical sensors employing superparamagnetic iron oxide (Fe_3O_4) nanoparticles with a surface functionalization of dimercaptosuccinic acid (DMSA) has been developed. The metal detection involves rapid collection of dispersed metal-bound nanoparticles from a sample solution at a magnetic or electromagnetic electrode, followed by the stripping voltammetry of the metal in acidic medium. The sensors were evaluated as a function of solution pH, the binding affinity of Pb to DMSA–Fe_3O_4, the ratio of nanoparticles per sample volume, preconcentration time, and Pb concentrations. The effect of binding competitions between the DMSA–Fe_3O_4 and urine constituents for Pb on the sensor responses was studied. After 90 s of preconcentration in samples containing 25 vol.% of rat urine and 0.1 g L^{-1} of DMSA–Fe_3O_4, the sensor could detect background level of Pb (0.5 ppb) and yielded linear responses from 0 to 50 ppb of Pb, excellent reproducibility (%RSD of 5.3 for seven measurements of 30 ppb Pb), and Pb concentrations comparable to those measured by ICP-MS. The sensor could also simultaneously detect background levels (<1 ppb) of Cd, Pb, Cu, and Ag in river and seawater.

Introduction

Large numbers of industrial workers are regularly exposed to toxic heavy metals like cadmium (Cd), lead (Pb), and mercury (Hg), which are known to induce various diseases that are detrimental to human health. Once in the body, the toxic metals will distribute to various tissue compartments (*e.g.*, liver, bone, and brain) and depending upon their pharmacokinetic properties (*i.e.* clearance rates, half-lives), a fraction of the metals will partition into the blood and may be excreted in urine. For Pb, the rate of urinary excretion is reported to be directly proportional to the plasma Pb concentration; hence, urinary Pb reflects Pb that has been cleared from the plasma to urine by the kidney.[1,2] Thus, urine is universally recognized as one of the best non-invasive matrices to assess exposures to a broad range of toxic metals.[3] Metal clearances in urine have also been correlated with the onset of various diseases, particularly those associated with renal function.[4] The state-of-the-art method for the analysis of Pb in urine is inductively coupled plasma-mass spectrometry (ICP-MS). The ICP-MS analyses are performed in laboratories, resulting in lengthy turn around time. Current established field-portable methods for Pb include NIOSH Methods 7700 (a screening method by spot test kits), 7701 (for analyzing lead in air filter samples using ultrasound/ASV), and 7702 (a field portable XRF for air samples on filters). According to NMAM, none of these methods have been established for Pb detection in biological matrices. The accuracy of Pb was reported to be about ±17–19% in nitric acid for the ultrasound/ASV technique, and ±16% on air filters for the portable XRF. The accuracy is likely to be worse in high complex biological matrices, thus for biomonitoring the accuracy must be improved. A portable analyzer employing an electrochemical technique will allow real-time analysis of metal ions in spot urine specimens, thereby representing a novel approach for the rapid assessment of exposure.

The major obstacles that prevent the wide applications of electrochemical sensors for analyzing metal ions in biological samples are (1) the binding of target metals to proteins,[5] leading to the low voltammetric response to known concentrations of the metals[6,7] and (2), the electrode fouling caused by proteins in the biological samples, leading to reduced signals and shorten the electrode life time. Adsorption of proteins at the solid–liquid interface is widely known,[8–13] even in samples containing extremely low protein content (*e.g.*, samples containing less than 1% of artificial saliva.)[10] For voltammetric detection of Cu in blood, the Compton group[11] has used solvent extraction coupled with

Pacific Northwest National Laboratory (PNNL), Richland, WA, 99352, USA. E-mail: wassana.yantasee@pnl.gov; Fax: +1 509-371-6242; Tel: +1 509-371-6265

ultrasound wave to free Cu from blood glycoproteins, followed by sonication during stripping voltammetric measurements of Cu (termed "sonoelectroanalysis"). For the detection of Pb in saliva, they have used the sonoelectroanalysis at a nafion coated mercury thin film electrode,[10] which evidently improved the detection of the trace Cu and Pb in the two fluids. However, large dilution factors of blood (*e.g.*, 2000-fold) and artificial saliva (*e.g.*, 40-fold) were required. Other researchers have explored the use of internal standards, such as indium[14] and thallium(III)[15] to compensate for the biological matrix effect on the blood Pb analysis at the Hg-film sensors. The use of internal standard increases measurement complexity, is less reliable when the ratio of Pb and the internal standard signal is not linear or resolution between the two peaks is poor, and thallium is known to be very toxic. Our previous work aimed at developing a portable electrochemical sensor for Pb in urine, blood, and saliva[16–18] has relied on acidifying the specimens to release Pb, followed by ultrafiltration to remove proteins and macromolecules from the specimens in combination with turbulent flowing of the Pb-contained specimens over Hg-film electrodes, which allowed us to successfully analyze Pb without matrix effect and electrode fouling. However, mercury-based electrodes have issues related to the use and disposal of toxic mercury, which may lead to its future regulation.

In developing mercury-free electrochemical sensors for metal detections, modifications of the sensor surface with bismuth films,[19,20] gold and platinum nanoparticles,[21,22] and a variety of chelating agents and sorbent materials[23–26] have been used for preconcentration of metal ions. However, these sensors still suffer from slow mass transport of the metal ions from bulk solution to the electrode surface. This is especially true in complex biological matrices in which metals are bound to organic molecules and proteins, thus, these Hg-free sensors are often not investigated for use in biological samples.

Recently, we have reported[27] a new class of highly dispersible sorbent material for environmental cleanup, the superparamagnetic iron oxide (Fe_3O_4) nanoparticles that are functionalized with dimercaptosuccinic acid (DMSA), which show extremely high affinity and selectivity for heavy metals, such as Pb, Cd, and Hg. Being magnetic, the metal-bound nanoparticles can be immobilized at a magnetic-based electrode surface prior to the voltammetic detection of the metal ions. This allows the preconcentration of Pb in urine to be done rapidly at open circuit without tedious sample pretreatment and adding electrolytes. With the use of DMSA–Fe_3O_4 as metal collector from biological samples, heavy metals like Pb can be directly detected in the samples using electrochemical sensors with high accuracy and sensitivity without (1) sample pretreatment by acid elution[16–18] or solvent extraction[11] to release metals from proteins into a pure medium followed by metal preconcentration at a mercury-film electrode, (2) the use of internal standards at Hg-based electrodes,[14,15] or (3) the use of sonication at the polymeric film-coated mercury–film electrode coupled with large sample dilution to minimize protein adsorption and promote mass transport of metals to the sensor surface.[10,11,28] Although our research focus is on urinary Pb analysis, we will also show the versatility of the DMSA–Fe_3O_4 based sensors in simultaneous detecting of multiple metals (Cd, Pb, Cu, and Ag) at as low as background levels in natural waters, which can be attributed to the high affinity of the DMSA for these metal ions.

Experimental

Sample preparation

Rat urine was collected from naïve male Sprague Dawley rats, 0.33–0.37 kg in weight, that were placed in glass metabolism cages designed for the separation of excreta. It was collected at 24 h intervals for a 72 h collection period (three samples per animal) on dry ice and stored frozen (−80 °C) until the Pb analysis was conducted. Since these rats were lab-grown, their urine did not contain sufficient Pb for a sensor optimization study. Thus, a pooled or individual rat urine was spiked with known amounts of Pb stock solution prepared from diluting of ICP standard solution (composed of 1000 mg L^{-1} of Pb in 1–2% HNO_3, Aldrich, Co) with DI water, incubated for at least 30 min to ensure the complete binding of Pb and urine constituents. Prior to the Pb detection, the Pb contained urine was diluted with DI water and DMSA–Fe_3O_4 suspension in DI water to obtain 4-fold dilution of Pb contained urine. For example, 0.125 mL of 100 ppb Pb-contained urine was mixed with 0.275 mL of DI and 0.1 mL of 0.5 g L^{-1} of DMSA–Fe_3O_4, which resulted in a sample containing 25 ppb of Pb, 25 vol.% of urine and 0.1 g L^{-1} of DMSA–Fe_3O_4. The preparation and surface characterization of DMSA–Fe_3O_4 were described elsewhere.[27] The solutions were used without adjusting pH (pH 8.5), except in the pH study where the solutions pH was adjusted with 1 M nitric acid.

K_d measurements

For the measurements of K_d as a function of pH, unfiltered seawater (Sequim Bay, WA, USA) was spiked with the Pb stock solution to obtain 500 ppb. The pH values of metal solutions were adjusted with nitric acid and sodium hydroxide to obtain the desired pH range. Each sample was then spiked with a small volume of known concentration of nanoparticles (suspended in DI water) to obtain a solid per liquid ratio (S/L in unit of g L^{-1} throughout) of 0.01. The sample was then agitated for 2 h at 160 rpm on an orbital shaker. After 2 h, each tube was then placed on the face of a 1.2 T Neodymium Iron Boron (NdFeB) magnet (K & J Magnetics, Inc., Jamison, PA, USA). All of the nanoparticles in the tube migrated toward the magnet in ~10 s. After 30–60 s, the supernatant was removed and kept in 1 vol.% HNO_3 prior to metal analysis. All batch experiments were performed in triplicates and the averaged values were reported. The concentrations of Pb before and after contacting with DMSA–Fe_3O_4 were measured by ICP-MS (Agilent 7500ce, Agilent Technologies, CA, USA) in accordance with the established procedure.[29] Similar K_d measurements were performed with multiple metal ions (500 ppb each of Cu, Ag, Cd, Hg, and Pb) in as-received river water (Columbia River, Richland, WA, USA) and seawater (Sequim Bay, WA, USA).

Magnetic and electromagnetic electrodes

Two classes of working electrodes were developed: a permanent magnetic electrode and an electromagnetic electrode. The

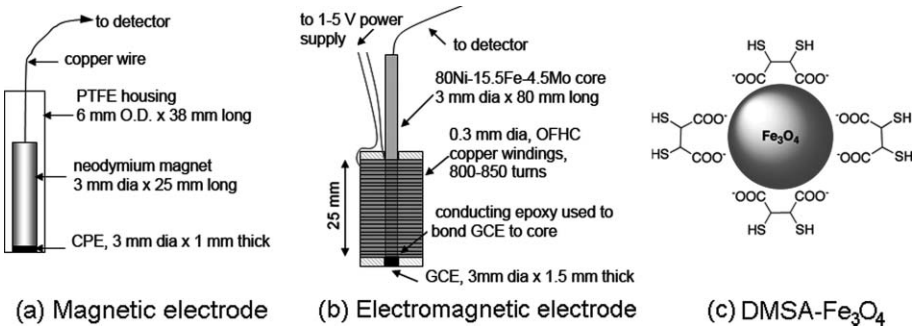

Fig. 1 Schematics of (a) magnetic electrode and (b) electromagnetic electrode which preconcentrate metal ions using (c) DMSA–Fe_3O_4 nanoparticles.

permanent magnetic electrode, as shown in Fig. 1(a), consisted of a neodymium cylinder magnet (3 mm dia. × 25 mm length, K & J Magnetics, Inc., Jamison, PA, USA) that was press-fit into a PTFE cylindrical tube (6 mm od × 38 mm length). The magnet was connected to a copper wire for electrical connection on one end. On the other end, it was packed with carbon graphite paste (Bioanalytical Systems, Inc.) to about 1 mm depth from the liquid interface. The surface of carbon paste was smoothed on a weighing paper and a very thin-layer was replaced after each measurement. The permanent magnetic electrode yielded the magnetic field strengths of 1700, 1000, 370, and 180 G, measured at 0, 1, 3, and 5 mm from the electrode–liquid interface.

The electromagnetic electrode, as shown in Fig. 1(b), consisted of a 3 mm dia. × 80 mm length ferromagnetic rod (80Ni–15.5Fe–4.5Mo, Goodfellow Corporation, Oakdale, PA, USA). Approximately 800–850 windings of oxygen-free high conductivity (OFHC) insulated copper wire (0.3 mm dia.) were wrapped over a 25 mm length of the rod near the electrode tip. The tip was made of glassy carbon (3 mm dia. × 1.5 mm depth) to minimize the physisorption of the nanoparticles which was found to be severe at the carbon paste electrode surface. When applying a current of 1.3 A (coil resistance of 2.3 Ω), the electromagnetic electrode yielded magnetic field strengths of 494, 320, 175, and 115 G, measured at 0, 1, 3, and 5 mm from the electrode–liquid interface.

Voltammetric detection

Square wave voltammetry (SWV) experiments were performed with a handheld electrochemical detector, model CHI1232A (CH Instruments, Inc., Austin, TX, USA), equipped with a three electrode system: a custom-made working electrode (Fig. 1(a–b)), a platinum wire as the auxiliary electrode, and Ag/AgCl in 3 M NaCl electrode as the reference electrode. Typical operating conditions are summarized in Table 1. During the metal preconcentration (normally for 90 s), the electrode tip was immersed into 0.5 mL of sample solution containing magnetic nanoparticles (DMSA–Fe_3O_4) and the solution was continuously shaken using a vortex mixer. After 90 s, the electrode tip was rinsed by stirring it for a few seconds in DI water to remove the residual sample (including the unbound Pb). During the rinsing, no nanoparticles were observed leaving the surface, owing to the strong magnetic field. Electrolysis was performed at −0.85 V for 60 s in 0.5 M acid solution (HNO_3 or HCl, both yielded no difference in Pb signals). After a 5 s quiet period at −0.7 V, the potential was scanned from −0.7 V to −0.35 V and the peak of Pb appeared at −0.56 V. All measurements were made at room temperature and under an atmospheric environment. All solutions were made of reagents of highest purity and were used without degassing. The SWV was operated at a frequency of 25 Hz with a pulse amplitude of 25 mV and a potential step height of 2 mV. For the permanent magnetic electrode, renewal of surface was performed by replacing a thin-layer of the carbon paste. For the electromagnetic electrode, cleaning was performed while the current to the copper coils was off (thus the electrode was no longer magnetic) and the potential of 0.6 V was applied for 60 s to the working electrode immersed in the stirred acid solution (same as the stripping solution), which completely removed both the nanoparticles and Pb.

In addition to urinary Pb analysis, to show the capability of the sensors in detecting multiple metal ions in natural waters, simultaneous detection of Cd, Pb, Cu, Ag, and Hg in as-received (non-filtered) river water (Columbia River, Richland, WA, USA) and seawater (Sequim Bay, WA, USA) were performed at the DMSA–Fe_3O_4-magnetic electrodes using the operating conditions as in Table 1. The concentrations of background and spiked metal ions in the waters were detected with both the DMSA–Fe_3O_4 sensors and ICP-MS for comparison.

Table 1 Typical operating conditions of DMSA–Fe_3O_4 based sensors

Parameters	Conditions
Sample	0.5 mL of Pb sample (25 vol.% urine) containing 0.1 g L^{-1} of DMSA–Fe_3O_4, pH 8.5
Preconcentration	90s in vortexed sample at open circuit
Electrolysis	−0.85 V, 60 s in 8 mL of 0.5 M HNO_3 or HCl
Detection	Scan from −0.70 V to −0.35 V in the same acid
SWV parameters	Amplitude: 25 mV, increment: 2 mV, frequency: 25 Hz

Results and discussion

Properties of DMSA–Fe_3O_4 nanoparticles

We have recently reported the surface properties of DMSA–Fe_3O_4 aimed at environmental cleanup.[27] In brief, the binding of DMSA ligands to the nanoparticle surface resulted in a change in water solubility of lauric acid-coated Fe_3O_4 nanoparticles that were completely insoluble to fully water-soluble. TEM images revealed an average diameter of DMSA–Fe_3O_4 particles utilized to be 5.8 ± 0.9 nm with little to no evidence of large

aggregate formation after suspending in an aqueous system. Brunauer, Emmett and Teller (BET) analysis revealed a surface area of 114 m^2 g^{-1}. Elemental analysis of S and Fe indicated that 1 g of the DMSA–Fe_3O_4 nanoparticles contained 0.80 ± 0.03 g (3.5 ± 0.1 mmol) of Fe_3O_4 and 0.16 ± 0.01 g (0.91 ± 0.05 mmol) of DMSA or 1.8 mmol of thiols, which is equivalent to full monolayer coverage. The IR spectrum showed the C = O stretches at ~1400 cm^{-1} and 1600 cm^{-1} and the S–H stretches at 2345 cm^{-1} and 2370 cm^{-1}. The carboxylate stretches were consistent with the carboxylate being bound to FeO surface, while thiol groups are free to bind with metal ions, as shown schematically in Fig. 1(c), which corresponded to the previous finding.[27,30] Three batches of DMSA–Fe_3O_4 were used to produce data for this manuscript. With good quality control of the nanoparticle synthesis, TEM and FTIR on each batch of the nanoparticles showed very little to no variation of the nanoparticle size and functional group attachment, resulting in no observed variation of Pb voltammetric analysis when other conditions were kept the same.

Pb binding competition between DMSA–Fe_3O_4 and urine constituents

Rat urine contains proteins/peptides, electrolytes, and metabolic byproducts, including 6200 ± 150 mg L^{-1} of urea, 210 ± 13 mg L^{-1} of uric acid, and 840 ± 44 mg L^{-1} of creatinine (from three 24 h urine specimens), assayed by colorimetric methods using analyte-specific QuantiChrom™ assay kits (BioAssay Systems, CA, USA). To effectively preconcentrate Pb, the DMSA–Fe_3O_4 must be able to effectively compete with these urine constituents for Pb. To study the binding kinetics of Pb to urinary constituents, the urine was spiked to obtain 100 ppb of Pb and incubated at room temperature for a specified period of time, followed by dilution of the sample 4-fold with DI water just prior to subjecting the sample to the DMSA–Fe_3O_4 based sensor. Fig. 2 shows that the peak signals of 25 ppb Pb decrease with increasing incubation time between Pb and urine from 0 to 10 min and level off thereafter. The decreased Pb signals are likely attributed to the binding of Pb to the urine constituents that results in a lower number of Pb that are free to bind with the DMSA–Fe_3O_4 and immobilized on the electrode surface. Fig. 2 also suggests that the steady-state binding occurs after 10 min. Thus to imitate real samples inherently containing Pb using urine spiked Pb, a 30 min incubation time was used throughout this study. Nevertheless, the sensors based on DMSA–Fe_3O_4 nanoparticles still provided highly sensitive detection of Pb in urine owing to their efficient metal preconcentration through suitable and dispersible binding sites followed by rapid magnetic collection at the electrode surface. To put things in perspective, the signal to noise of 25 ppb Pb in 25 vol.% urine measured at the DMSA–Fe_3O_4 based sensors was comparable to that of 100 ppb Pb in DI water measured at the carbon paste electrode immobilized with a thiol-functionalized sorbent.[31]

Effect of solution pH

Fig. 3 shows the effect of solution pH on the Pb signals measured in solutions containing 30 ppb Pb, 25 vol.% rat urine, and 0.1 g DMSA–Fe_3O_4 L^{-1}. Fig. 3 also shows the distribution coefficients (K_d) of Pb, measured in pH adjusted sea water (S/L of 0.01 g DMSA–Fe_3O_4 L^{-1}). The voltammetric signals of Pb are controlled by how well the DMSA–Fe_3O_4 can capture Pb and are subsequently collected on the electrode surface. The extent of Pb capture is represented by the K_d; the higher the K_d, the higher affinity of the sorbent for the metal ion is. From pH about 0 to 5, the K_d values were small, corresponding to virtually no Pb signals in that pH range. As pH increased from about 5 to 8, the K_d values increased significantly, corresponding to substantial increases in Pb signals. Above pH 8, the K_d appeared to decrease and so did the Pb signals, which dropped more drastically than the K_d. Although the optimal pH was found to be 7.6, the detection sensitivity of Pb in normal rat urine (pH ~ 8.5 after 4-fold dilution in DI) is still large in this concentration range. Thus, for user-friendly use of the sensors, no pH adjustment is required. Unless specified otherwise, the urine samples were used without pH adjustment throughout.

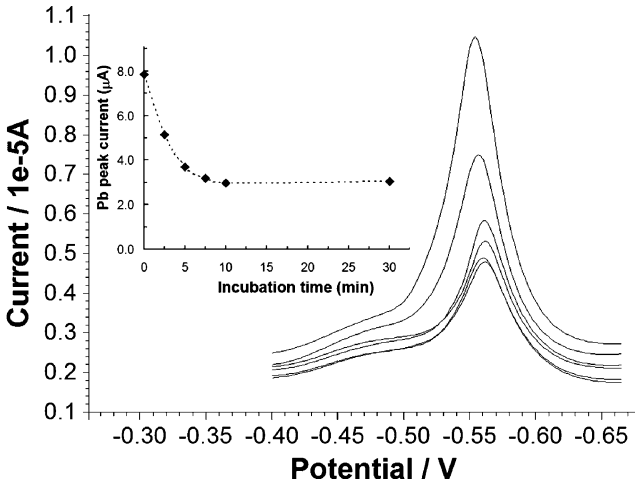

Fig. 2 Voltammograms of 25 ppb Pb measured at DMSA–Fe_3O_4-magnetic sensors in decreasing order with increasing incubation time between Pb and rat urine. Inset is the Pb signal *vs.* incubation time profile; other operating conditions as in Table 1.

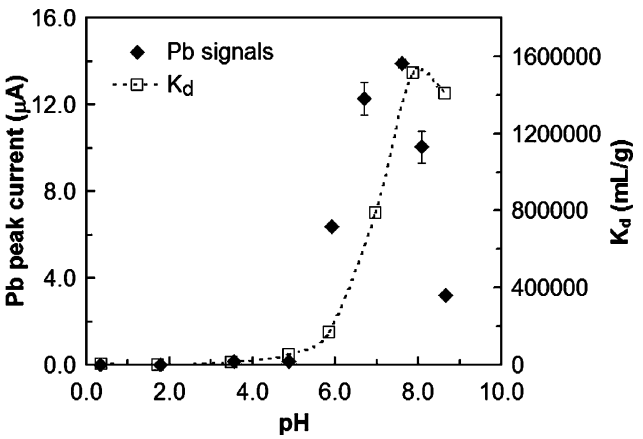

Fig. 3 Signals of 30 ppb Pb measured at DMSA–Fe_3O_4-magnetic sensors in pH-adjusted samples containing 25 vol.% of rat urine; other operating conditions as in Table 1. Right-hand *Y*-axis shows the distribution coefficient (K_d) of Pb, measured in pH-adjusted seawater.

Effect of S/L

Fig. 4 shows the effect of the nanoparticle content (S/L in g DMSA-Fe_3O_4 L^{-1} of solution) on the signals of 10 ppb Pb, measured in solutions containing 25 vol.% of rat urine. Without the nanoparticles, no Pb peak was observed even when the samples contained 250 ppb Pb and 25% urine (or 1000 ppb in whole urine). This is because the carbon paste alone could not precontrate Pb (*e.g.*, not able to compete with urine constituents for binding with Pb). The peak current of Pb increased linearly as the content of DMSA–Fe_3O_4 increased from 0.001 g L^{-1} to 0.33 g L^{-1}. More nanoparticles offer more binding sites to immobilize Pb on the sensor surface resulting in higher Pb signals. For economical use of the nanoparticles, an S/L of 0.1 g L^{-1} was sufficient for detecting Pb in this concentration range (10 ppb). Even at high S/L of 0.33 g L^{-1}, the surface was not saturated by the nanoparticles, suggesting that a very low detection limit can be obtained with increasing the amount of the nanoparticles in the solutions.

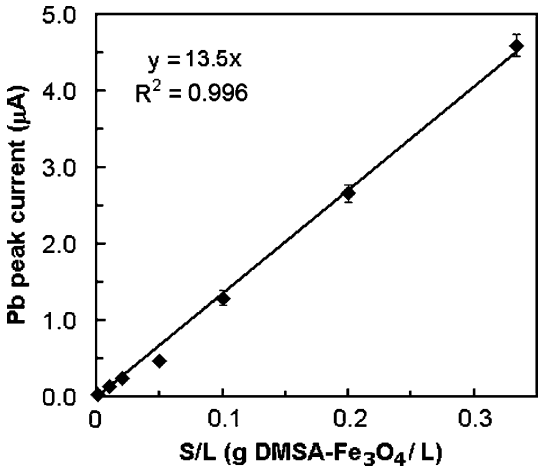

Fig. 4 Signals of 10 ppb Pb measured at DMSA–Fe_3O_4-magnetic sensors in samples containing 25 vol.% of rat urine with varied concentrations of DMSA-Fe_3O_4; other operating conditions as in Table 1.

Effect of preconcentration time

Fig. 5 shows the effect of preconcentration time on the peak signals of 10 ppb Pb in solution containing 25 vol.% of rat urine and 0.1 g L^{-1} of DMSA–Fe_3O_4. The nanoparticles were added to the solution immediately prior to immersing the electrode into the solution, thus the time that the nanoparticles were allowed to capture Pb coincides with the magnetic collection time of the nanoparticles on the electrode surface, which is defined as the preconcentration time. In Fig. 5, the Pb signals increased as the preconcentration time increased from 0 to 150 s and leveled off at above 150 s. Since the data in Fig. 4 suggests that the electrode surface is not easily saturated by the nanoparticles, the leveling of peak current is evidence of complete collection of the nanoparticles from the solutions onto the electrode surface. The ability to collect nanoparticles of this small size (6 nm) from solutions with a relatively low magnetic field gradient suggests that the nanoparticles formed aggregates under the applied field gradient, which is believed to be reversible once the

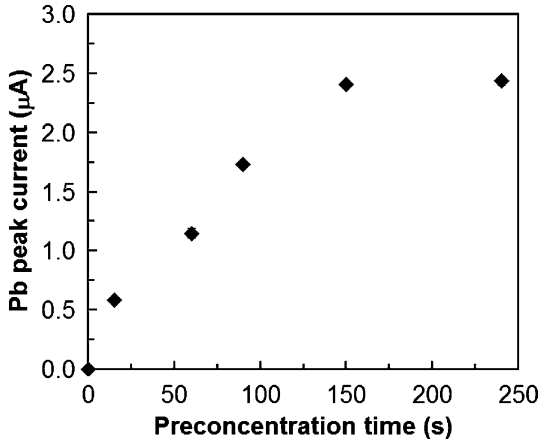

Fig. 5 Signals of 10 ppb Pb measured at DMSA–Fe_3O_4-magnetic sensors in samples containing 25 vol.% of rat urine with varied preconcentration time; other operating conditions as in Table 1.

field is removed as demonstrated in a recent work.[30] For rapid analysis, 90 s was found sufficient to detect Pb in the low ppb range (*e.g.* 10 ppb). In addition to fast magnetic collection, the short preconcentration time is also due to the easy accessibility of Pb ions to the binding sites (DMSA) which are coated on the exterior surface of the nanoparticles, unlike porous materials having the binding sites attached to the pore walls.[27] The lack of internal diffusion resistance of the nanoparticles is very beneficial especially when the metal ions are bound to large molecules like many urine constituents.

Effect of Pb concentration

Fig. 6 shows the Pb signals as a function of concentrations of Pb in the solutions containing 25 vol.% of rat urine and 0.1 g L^{-1} of DMSA–Fe_3O_4. The linear response was obtained from 0 to 50 ppb of Pb in a sample containing 25 vol.% urine, which is equivalent to 0 to 200 ppb of Pb in whole urine. This concentration range is relevant to urinary biomonitoring of Pb for both normal and exposure levels. For example, Biological Exposure Index (BEI), based on 1994–1995 Recommendations of the American Conference of Governmental Industrial

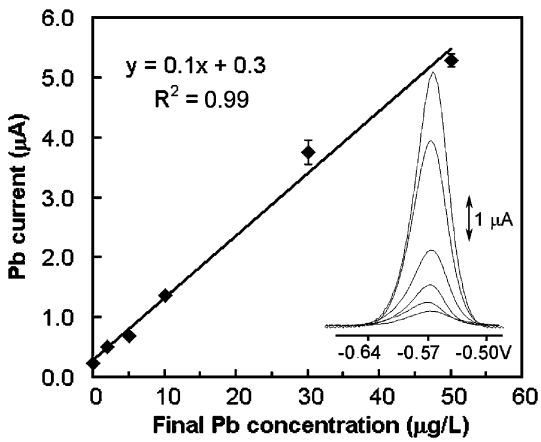

Fig. 6 Linear Pb calibration curve measured at DMSA–Fe_3O_4-magnetic sensors in Pb-spiked samples containing 25 vol.% of rat urine; other operating conditions as in Table 1.

Hygienists (ACGIH) of Pb in spot urine is 150 μg g^{-1} of creatinine, which is equivalent to 200 ppb of Pb (assuming normal values of 2 g of creatinine[32] and 1.5 L of urine excreted per day).[33] After EDTA infusion, a Pb excretion rate over 50 μg in 24 h urine suggests an increased body burden as a result of past exposure to Pb.[34]

Validation

Fig. 7 shows the signals of Pb from three urine specimens that were collected from 3 individual rats and spiked with Pb. It shows a clear evidence of the matrix effect on the Pb signals which may be due to the varied degree of diluteness of the as-received specimens. Therefore, the metal content in urine is generally reported with creatinine normalization. However, creatinine measurement is beyond the scope of this manuscript. Thus a standard addition method was used to obtain the concentration of Pb in the three urine specimens as shown in Table 2. The Pb concentration in whole urine was the absolute value of *X*-intercept (derived from *Y*-intercept divided by the slope) that was corrected for the dilution factors (by 4 to 5 fold). The Pb concentrations obtained with the DMSA–Fe_3O_4 based sensors compare very well with those measured by ICP-MS as summarized in Table 2.

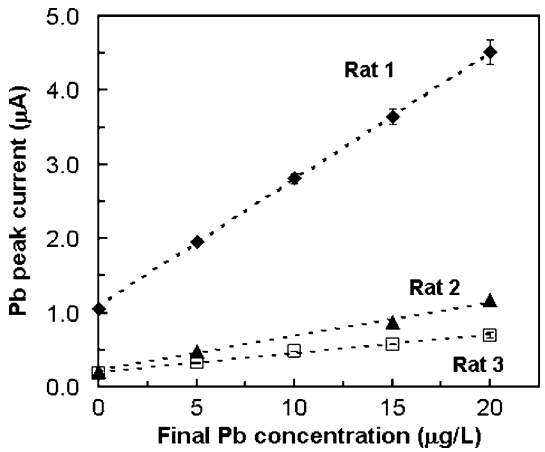

Fig. 7 Pb signals by standard addition method measured at DMSA–Fe_3O_4-magnetic sensors in Pb-spiked samples contained 25 vol.% of urine from three individual rats; other operating conditions as in Table 1.

Table 2 Pb concentrations in three rat urine specimens measured with DMSA–Fe_3O_4 sensors by a standard addition method and ICP-MS

Parameters	Rat 1	Rat 2	Rat 3
Slope/μA ppb^{-1} Pb	0.17	0.05	0.03
Y-intercept/μA	1.08	0.23	0.20
X-intercept (ppb of Pb in diluted urine sample)[a]	6.3	4.9	7.7
Pb in whole urine[b] (ppb)	25.1	19.7	38.5
Pb by ICP-MS analysis (ppb)	25.0	20.1	41.4
Deviation from ICP-MS values (%)	0.2	1.8	7.0

[a] Absolute of *X*-intercept = *Y*-intercept/slope. [b] Absolute of *X*-intercept × dilution factor (4× for specimens from Rat 1 and 2, and 5× from Rat 3).

Reproducibility and detection limits

The DMSA–Fe_3O_4 based sensors could detect Pb in samples containing rat urine with excellent reproducibility; seven measurements of 30 ppb Pb in samples containing 25 vol.% rat urine yielded a relative standard deviation of 5.3% (RSD, data not shown). The sensors have excellent detection limits; they could detect background Pb in rat urine (~0.5 ± 0.2 ppb by ICP-MS, 4 samples) even after 4-fold dilution and 2.5 ppb Pb spiked urine samples (Fig. 6) after 90 s of preconcentration.

Multiple metal detection in natural waters

The DMSA–Fe_3O_4 nanoparticle is a versatile sorbent that has high affinity not only for Pb, but also for other soft metals. Fig. 8(a) shows that, when used in as-received Columbia River water and Sequim Bay seawater, the DMSA–Fe_3O_4 based sensors could detect background Cd, Pb, Cu, and Ag which in some case (*e.g.*, the case of Pb in river water) was lower than the detected limits (~0.008 ppb Pb) of the state of the art ICP-MS (see inset of Fig. 8(a)). The inset also shows the binding affinity (K_d) of DMSA–Fe_3O_4 to various metal ions in

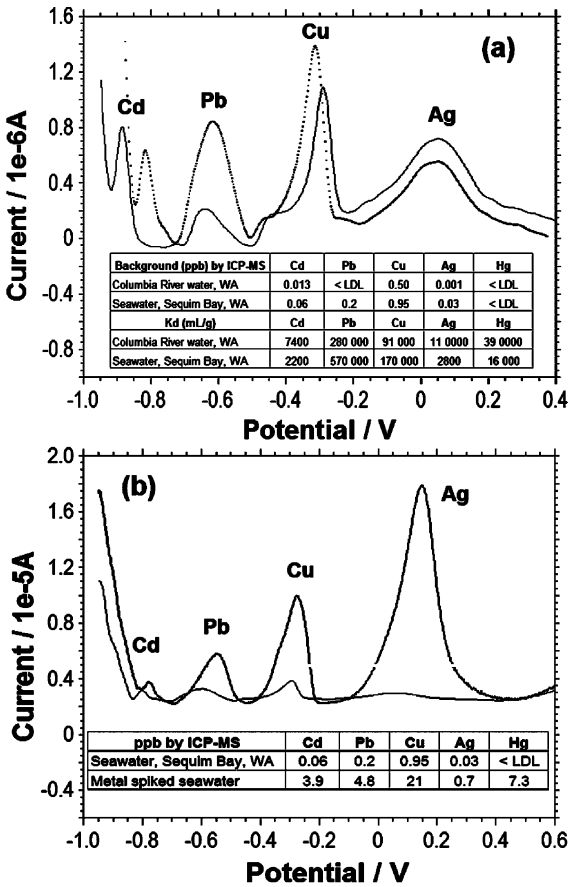

Fig. 8 Sensor measurements of (a) background metal ions in seawater (dashed line) and river water (solid line) and (b) background metal ions (thin line) and metals spiked (thick line) in seawater, after 150 s of preconcentration time; other operating conditions as in Table 1. Inset shows the metal concentrations, measured with ICP-MS, and the distribution coefficients of multiple metal ions (S/L of 0.01 g L^{-1} of DMSA–Fe_3O_4, initial metal conc. of 500 ppb each, pH of 7.20 for river water and 7.64 for seawater).

the river water and seawater. From the K_d values, the DMSA–Fe_3O_4 nanoparticles are an outstanding sorbent for Hg, Ag, Pb, and Cu (K_d > 50 000 mL g^{-1})[35] in river waters, and for Cu and Pb in seawater. Although DMSA–Fe_3O_4 has a high K_d for Hg, Hg could not be detected due to its strong binding between Hg and DMSA in the acidic stripping solution,[27] thus Hg could not be released from the nanoparticles and reduced onto the electrode surface. For a specific metal, its signal strength not only depends on the concentration of the metal present in the waters, but also on the affinity (K_d) of the DMSA–Fe_3O_4 for that metal. For example, although Ag concentration in seawater was higher than that in river water, the lower K_d value of Ag in seawater (due to the formation of negatively charged Ag–Cl complexes)[36] resulted in a Ag peak that was not larger than that in river water. Fig. 8(b) shows the responsiveness of the sensors when metals were spiked into seawater in comparison to the as-received seawater; the responsiveness is in the decreasing order of Ag > Pb > Cu > Cd > Hg.

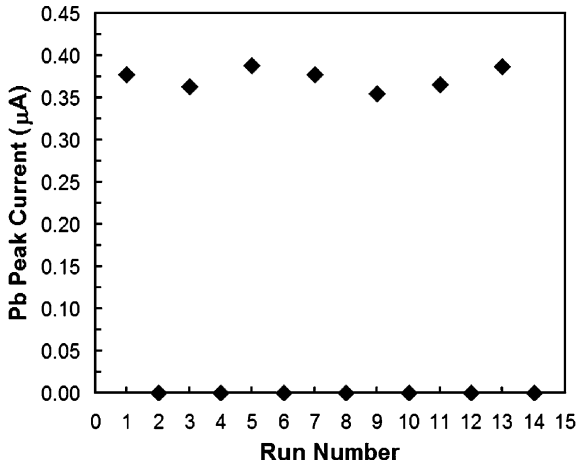

Fig. 9 Measurements of 10 ppb Pb in seawater at a DMSA–Fe_3O_4-electromagnetic sensor, with 1.3 A current on (odd-number runs) and off (even-number runs) during 90 s preconcentration; other operating conditions as in Table 1.

Automation

Due to the strong magnetic field, the permanent magnet sensor did not allow the release of DMSA–Fe_3O_4 from the electrode surface once a measurement was done, thus the surface must be manually renewed by replacing a thin layer of the carbon paste. Toward automation of the detection, we have developed an electromagnetic electrode (Fig. 1(b)). By turning the current to the copper coils on and off, capturing of the nanoparticles at the electrode surface and releasing them could be accomplished without manual surface renewal. Fig. 9 shows the signals for 10 ppb Pb measured in seawater with S/L of 0.1 g L^{-1} of DMSA–Fe_3O_4. The odd number runs were measured after the current to the copper coils was on for 90 s during the preconcentration of Pb (*e.g.*, the electrode was immersed in stirred Pb solutions containing DMSA–Fe_3O_4), while the even number runs were measured after the current was off during the 90 s of preconcentration. After the preconcentration, electrolysis and detection were performed while the current was on and with the conditions in Table 1. Regeneration of the electrode was performed while the current to the copper coils was off and the potential of 0.6V was applied to the working electrode for 60 s in the stirred acid solution. Fig. 9 suggests that there is no memory effect of the electromagnetic electrode from one measurement to the next and that it can be fully regenerated. The electrode has good sensitivity; after only 90 s of preconcentration, it could detect 10 ppb of Pb in seawater, the concentration that is lower than the EPA's action level of Pb (15 ppb) in public drinking water supplies.[37] It has excellent reproducibility; the %RSD of 8 consecutive measurements of 10 ppb Pb in seawater was 4.1%. More results on automated electromagnetic sensors will be reported in due course.

Conclusions

Electrochemical sensors based on DMSA functionalized magnetic nanoparticles can overcome the fouling and competition for Pb by urinary constituents, both of which are major obstacles preventing successful electrochemical detection of metal ions in biological matrices. The nanoparticles enabled direct detection of Pb in urine in the relevant range (0 to 200 ppb) of Pb biomonitoring. The optimal operating conditions involved a 90 s preconcentration with 0.1 g L^{-1} of DMSA–Fe_3O_4 in samples containing 25 vol.% of urine, electrolysis at −0.85 V for 60 s in a 0.5 M acid solution, and SWV detection of the metal in the same acid solution. The sensors were very sensitive and could detect background Pb (0.5 ppb Pb) in samples containing 25 vol.% of rat urine. They yielded urinary Pb concentrations that were comparable to those measured by the ICP-MS. They could also simultaneously detect background levels (<1 ppb) of Cd, Pb, Cu, and Ag in natural waters. In addition to excellent detection sensitivity, accuracy, and reproducibility, the sensors have great potential to be portable and field-deployable monitoring tools for toxic metals because (1) they require no toxic mercury for metal preconcentration, (2) they require no pH adjustment and no sample pretreatment except small-factor dilution, (3) they can be automated by exploiting electromagnetic field in collecting and no field in releasing the magnetic nanoparticles from the electrode surface, (4) the magnetic nanoparticles are highly dispersible and become homogeneous with samples, thus the sensing process can be easily automated, (5) they have high throughput (~3 min per sample), and (6) they have economic uses of samples (0.5 mL) and nanoparticles (0.05 mg) per measurement, thereby generating less waste.

Acknowledgements

This work was supported by grant 1R21 OH008900–01 from NIOSH and by the PNNL's Laboratory Directed Research and Development. Its contents are solely the responsibility of the authors and do not necessarily represent the official views of NIH. The research was performed in part at the Environmental Molecular Sciences Laboratory (EMSL), a DOE national scientific user facility located at PNNL. The authors thank Dr Joongjai Panpranot, Dr Karla Thrall, Andrea L. Busby, John S. Rohrer, Robert L. Workman, and Jolen Soelberg for their contributions.

References

1 J. Barbosa, J. Eduardo Tanus-Santos, R. Fernanda Gerlach and P. Parson, *Environ. Health Perspect.*, 2005, **113**, 1669–1674.
2 E. O'Flaherty, *Crit. Rev. Toxicol.*, 1998, **28**, 271–317.
3 Z. Karpas, A. Lorber, E. Elish, P. Marcus, Y. Roiz, R. Marko, R. Kol, D. Brikner and L. Halicz, *Health Phys.*, 1998, **74**, 86–90.
4 H. Roels, P. Hoet and D. Lison, *Renal Failure*, 1999, **21**, 251–262.
5 Y. Lin, R. Zhao, K. D. Thrall, C. Timchalk, W. D. Bennett and M. D. Matson, *Proc. SPIE–Int. Soc. Opt. Eng.*, 1999, **3877**, 248.
6 C. Timchalk, T. S. Poet, Y. Lin, K. K. Weitz, R. Zhao and K. D. Thrall, *Am. Ind. Hyg. Assoc. J.*, 2001, **62**, 295–302.
7 J. Wang, *J. Electroanal. Chem.*, 1982, **139**, 225.
8 C. E. Bohs, M. C. Linhares and P. T. Kissinger, *Curr. Sep.*, 1994, **13**, 6.
9 D. T. Kim, H. W. Blanch and C. J. Radke, *Langmuir*, 2002, **18**, 5841.
10 C. E. West, J. L. Hardcastle and R. G. Compton, *Electroanalysis*, 2002, **14**, 1470–1478.
11 J. L. Hardcastle and R. G. Compton, *Electroanalysis*, 2002, **14**, 753–759.
12 J. L. Hardcastle, G. G. Murcott and R. G. Compton, *Electroanalysis*, 2000, **12**, 559.
13 J. L. Hardcastle, C. E. West and R. G. Compton, *Analyst*, 2002, **127**, 1495.
14 T. Z. Liu, D. Lai and J. D. Osterloh, *Anal. Chem.*, 1997, **69**, 3539–3543.
15 C.-C. Yang, A. S. Kumar and J.-M. Zen, *Anal. Biochem.*, 2005, **338**, 278–283.
16 W. Yantasee, C. Timchalk, K. K. Weitz, D. A. Moore and Y. Lin, *Talanta*, 2005, **67**, 617–624.
17 W. Yantasee, C. Timchalk and Y. Lin, *Anal. Bioanal. Chem.*, 2007, **387**, 335–341.
18 W. Yantasee, Y. Lin, K. Hongsirikarn, G. Fryxell, R. Addleman and C. Timchalk, *Environ. Health Perspect.*, 2007, **115**(12), 1683–1690.
19 C. Gouveia-Caridade, R. Pauliukaite and C. M. A. Brett, *Electroanalysis*, 2006, **18**, 854–861.
20 G. Liu, Y. Lin, Y. Tu and Z. Ren, *Analyst*, 2005, **130**, 1098–1101.
21 X. Dai, O. Nekrassova, M. E. Hyde and R. G. Compton, *Anal. Chem.*, 2004, **76**, 5924–5929.
22 X. Dai and R. G. Compton, *Analyst*, 2006, **131**, 516–521.
23 A. Walcarius, *Chem. Mater.*, 2001, **13**, 3351–3372.
24 Y. Lin, W. Yantasee, G. E. Fryxell, Electrochemical sensors based on functionalized nanoporous silica, *Dekker Encyclopedia of Nanoscience and Nanotechnology*, Marcel Dekker, New York, 2004, pp. 1051–1062.
25 A. J. Tchinda, E. Ngameni and A. Walcarius, *Sens. Actuators, B*, 2007, **121**, 113–123.
26 M. Trojanowicz, *Microchim. Acta*, 2003, **143**, 75–91.
27 W. Yantasee, C. L. Warner, T. Sangvanich, R. S. Addleman, T. G. Carter, R. J. Wiacek, G. E. Fryxell, C. Timchalk and M. G. Warner, *Environ. Sci. Technol.*, 2007, **41**, 5114–5119.
28 J. Kruusma, L. Nei, J. L. Hardcastle, R. G. Compton, E. Lust and H. Keis, *Electroanalysis*, 2004, **16**, 399–403.
29 Agilent-Technologies, Method 5988–0533EN, Determination of heavy metals in whole blood by ICP-MS, 2006.
30 C. T. Yavuz, J. T. Mayo, W. W. Yu, A. Prakash, J. C. Falkner, S. Yean, L. Cong, H. J. Shipley, A. Kan, M. Tomson, D. Natelson and V. L. Colvin, *Science*, 2006, **314**, 964–967.
31 W. Yantasee, Y. Lin, T. S. Zemanian and G. E. Fryxell, *Analyst*, 2003, **128**, 467–472.
32 T. W. Demant and E. C. Rhodes, *Sports Med.*, 1999, **28**, 49–60.
33 M. Lever, W. Atkinson, P. C. B. Sizeland, S. T. Chambers and P. M. George, *Clin. Biochem.*, 2007, **40**, 447–453.
34 M. Markowitz, *Curr. Probl. Pediatr.*, 2000, **30**, 62–70.
35 G. E. Fryxell, Y. Lin, S. Fiskum, J. C. Birnbaum, H. Wu, K. Kemner and S. Kelly, *Environ. Sci. Technol.*, 2005, **39**, 1324–1331.
36 R. H. Byrne, *Geochem. Trans.*, 2002, **3**, 11–16.
37 EPA, Technical Factsheet on: LEAD, http://wwwepagov/OGWDW/dwh/t-ioc/leadhtml.